frontiers | Frontiers in Earth Science

TYPE Original Research
PUBLISHED 16 September 2024
DOI 10.3389/feart.2024.1441323

OPEN ACCESS

EDITED BY
Nadia Solovieva,
University College London, United Kingdom

REVIEWED BY
Rienk H. Smittenberg,
Snow and Landscape Research (WSL), Switzerland
Yafei Zou,
Zhengzhou University, China

*CORRESPONDENCE
Kaitlyn E. Horisk,
keh5809@psu.edu
Sarah J. Ivory,
sji15@psu.edu

RECEIVED 30 May 2024
ACCEPTED 28 August 2024
PUBLISHED 16 September 2024

CITATION
Horisk KE, Ivory SJ, Freeman KH, Baczynski AA, McCorriston J, Anderson A, Anderson RS and Al-Kathiri A (2024) Late Holocene hydrologic variability and ecosystem structure from rock hyrax middens in Dhofar, Oman.
Front. Earth Sci. 12:1441323.
doi: 10.3389/feart.2024.1441323

Late Holocene hydrologic variability and ecosystem structure from rock hyrax middens in Dhofar, Oman

Kaitlyn E. Horisk[1]*, Sarah J. Ivory[1,2]*, Katherine H. Freeman[1], Allison A. Baczynski[1,3], Joy McCorriston[4], Andrew Anderson[5], R. Scott Anderson[6] and Ali Al-Kathiri[7]

[1]Department of Geosciences, Penn State University, University Park, PA, United States, [2]Earth and Environmental Systems Institute, Penn State University, University Park, PA, United States, [3]Laboratory for Isotopes and Metals in the Environment (LIME), Penn State University, University Park, PA, United States, [4]Department of Anthropology, The Ohio State University, Columbus, OH, United States, [5]The Royal Botanic Garden, Edinburgh, United Kingdom, [6]School of Earth and Sustainability, Northern Arizona University, Flagstaff, AZ, United States, [7]The Ministry of Heritage and Tourism, Muscat, Oman

Over 1/3 of the Earth's human population relies on dryland ecosystems for food and water resources. While these ecosystems are highly sensitive to changes in climate, we lack observational data as to how changes in hydrology influences plant communities. Paleoecological data for southern Arabia show woodland communities transitioned to more dry-adapted herbaceous plants, which suggests rainfall decreased across the Holocene. To assess relationships between hydrology and ecology, we employed leaf wax *n*-alkane distributions, $\delta^{13}C_{wax}$, and δD_{wax} records from rock hyrax (*Procavia capensis*) middens in Dhofar, Oman. The biomarker properties allowed reconstruction of changes in C3/C4 vegetation and local moisture availability, in tandem with community changes represented by a published pollen record. To constrain interpretations, *n*-alkane analyses were conducted on herbarium specimens of leaves collected in Dhofar. For the modern specimens, xeric plants typically contained longer homologues than mesic plants. Across the fossil middens (4,038–109 cal yrs BP), the proportions of plant-wax homologues do not show major changes, and thus do not suggest a shift between xeric versus mesic plants. Similarly, $\delta^{13}C_{wax}$ values indicate little or no change in the distributions of C3 and C4 vegetation. Limited δD_{wax} data from the middens confirm overall drying occurred into the late Holocene, punctuated by a wetter pulse at ~1.6 ka. Taken together, plant wax distributions and isotope data indicate changes in moisture availability across the late Holocene did not alter the structural composition of the plant communities and that the proportion of C3/C4 vegetation remained stable. We infer vegetation changes associated with late Holocene drying involved reshuffling of community composition and not major changes in vegetation structure. Additionally, this study demonstrates that leaf wax *n*-alkanes from rock hyrax middens provide a method to reconstruct changes in climate and vegetation in dryland ecosystems where other archives are scarce.

KEYWORDS

n-alkanes, isotopes, geochemistry, paleoecology, hydrology, rock hyrax middens

1 Introduction

Drylands are regions where potential evaporation outpaces annual precipitation by at least 1.5-fold. These arid landscapes are found on every major continent and support over 40% of the Earth's population. Global climate models predict an overall increase in aridity globally due to changes in rainfall as well as increased evapotranspiration from higher temperatures (Asner et al., 2004; Maestre et al., 2016; Dahinden et al., 2017; IPCC, 2022). Predicted higher variability in rainfall as well as an increase in extreme events such as droughts are expected to also stress dryland ecosystems (Asner et al., 2004; Maestre et al., 2016; IPCC, 2022). Decreases in rainfall have a significant impact on vegetation density in arid places (Maestre et al., 2016). Studies suggest 10%–20% of drylands are already severely degraded, and as aridity intensifies with climate warming, the resulting altered species composition and reduced vegetation cover will impact the availability of food, fodder and lumber to hundreds of millions of people (Asner et al., 2004; Maestre et al., 2016; Ball and Tzanopoulos, 2020).

The Dhofar region of Oman is a biodiverse dryland that is home to cloud forest woodlands, which rely on moisture from dense fog brought in seasonally by the Indian Monsoon (Fleitmann et al., 2007; Hildebrandt et al., 2007; Friesen et al., 2018). These woodlands are both ecologically and economically important; they serve as a critical resource for both people and animals (El-Mahi, 2011; Hildebrandt et al., 2007; Ball and Tzanopoulos, 2020). More broadly, vegetation across Dhofar provides grazing resources for domesticate animals, particularly camels (McCorriston et al., 2020). This region is expected to enter novel climate space by the end of this century (Dahinden et al., 2017), and large-scale changes in vegetation have already occurred in this region over the last few decades. For example, cloud forest woodlands have contracted in space and have been degraded over the last few decades due to increased human land use (El-Mahi, 2011; Ball and Tzanopoulos, 2020; McCorriston et al., 2020).

Modern observational data are too brief to assess long-term trends in climate change and vegetation response. While modern data can assess the impacts of extreme events on vegetation, which generally occur in a timeframe of months to a few years, anthropogenic climate change will occur over decades to centuries, thus more data are needed to capture these long-term dynamics (Dietl et al., 2014; Afuye et al., 2021). Paleoenvironmental records can be used to understand these relationships over long periods of time. Regional paleoclimate studies generally agree that rainfall decreased across the Holocene in northern Africa and southern Arabia as the Indian Monsoon system weakened (Morrill et al., 2003; Renssen et al., 2003; Fleitmann et al., 2007; Böll et al., 2014; Lézine et al., 2014; Nicholson, 2018). However, there are currently very few paleoecological records investigating climate-vegetation dynamics in southern Arabia (Lézine et al., 2002; Lézine et al., 2017; Ivory et al., 2021; Hoorn and Cremaschi, 2004).

In southern Arabia from the mid to late Holocene, vegetation responses to increased aridity are described by pollen records that are patchy in both space and time. Pollen studies from paleolakes and hyrax middens from nearby Yemen suggest a contraction of semi-arid woodlands inland across the Holocene (Lézine et al., 2017; Ivory et al., 2021). Most paleoenvironmental data from Oman comes from speleothem records or sediment core records from the coast (Hoorn and Cremaschi, 2004; Fleitmann et al., 2007; Lippi et al., 2007; Bellini et al., 2022; Horisk et al., 2023). Omani mangrove records demonstrate an increase in xeric, saline-tolerant taxa on the coast over this time frame (Lézine et al., 2002). Oxygen isotopes from the speleothems indicate an overall trend of decreasing rainfall across the Holocene, while sedimentological information from the estuarine records highlights wetter pulses that punctuate this long-term trend, characterized by higher sediment inputs from more surface runoff (Hoorn and Cremaschi, 2004; Fleitmann et al., 2007; Lippi et al., 2007; Bellini et al., 2022). Given the sparse data, the impact of long-term changes in precipitation on vegetation further inland in this region is not well-understood.

Rock hyrax middens serve as a powerful paleoecological archive in arid regions which lack more traditional archives such as lakes or bogs. Pollen studies from hyrax middens in both Africa and Arabia have successfully reconstructed ancient vegetation change across the Holocene and late Pleistocene (Scott and Cooremans, 1992; Chase et al., 2012; Ivory et al., 2021; Horisk et al., 2023). A pollen record from rock hyrax middens in Dhofar demonstrated changes in vegetation in the inland desert (Nejd) across the late Holocene (Horisk et al., 2023), indicating an overall shift to more xeric, herbaceous taxa at ~1.6 ka. More recent explorations of geochemical tools within the middens have demonstrated the efficacy of bulk stable isotopes in assessing past changes in vegetation and moisture as well as leaf wax biomarkers (Carr et al., 2010; Chase et al., 2012; Carr et al., 2016). Herein lies an opportunity to develop a long-term paleoecological record to disentangle climatic drivers of vegetation change in an inland, biodiverse dryland community.

1.1 Modern environment

The Dhofar region is semiarid on the coast (~120–150 mm/yr) to hyperarid further inland in the desert (~30 mm/yr). The vegetation is highly biodiverse: at least 817 species have been documented in Dhofar alone, many of which are endemic, and this represents over half of the total flora in the county (Patzelt, 2015). Moreover, it is estimated that nearly 14% of the total vegetation in Oman is range-restricted, and thus at increased risk under changing climate conditions (Patzelt, 2015). The vegetation is highly dependent on the annual precipitation, which comes mainly from the Indian Monsoon system (Miller and Morris, 1988; Fleitmann et al., 2007; Hildebrandt et al., 2007; Ball and Tzanopoulos, 2020).

The vegetation in the Dhofar region is composed of four ecological zones from the Arabian Sea inland: the coastal plain, the escarpment, the plateau, and the Nejd (Figure 1; Miller and Morris, 1988). The coastal plain today is sparsely vegetated due to grazing of domesticate animals and other human land use such as urbanization and infrastructure (Miller and Morris, 1988; El-Mahi, 2011). Near estuaries, vegetation is dominated by grasses (Poaceae), some sedges (Cyperaceae), *Salvadora persica* trees, and semi-aquatic plants such as *Typha* (Ghazanfar, 1999; McCorriston et al., 2018). The escarpment sharply increases in elevation and is home to a semiarid cloud forest (Miller and Morris, 1988; Patzelt, 2015; Ball and Tzanopoulos, 2020). This unique woodland can intercept fog brought in by the Indian Monsoon and flourishes seasonally (Hildebrandt et al., 2007; Friesen et al., 2018).

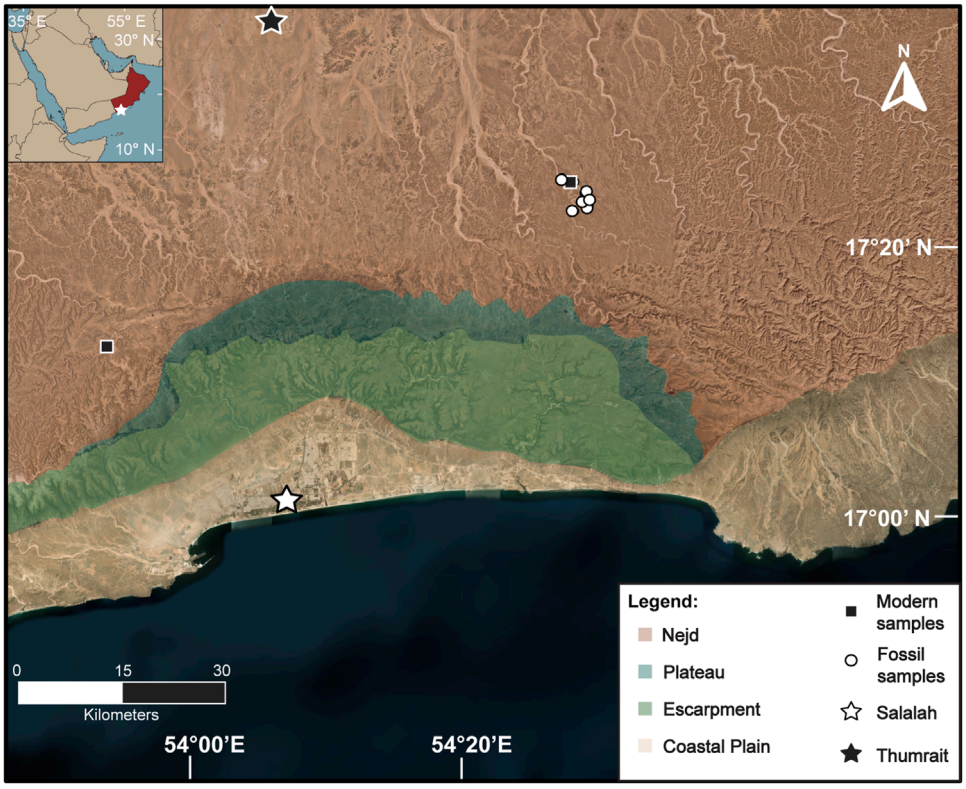

FIGURE 1
Map of the Dhofar region indicating the four ecological zones. Black squares are modern samples, white circles represent fossil samples. The stars denote the weather stations in Salalah and Thumrait. Modified from Horisk et al. (2023).

This community consists of trees that require seasonal moisture such as *Terminalia dhofarica*, *Maytenus dhofarensis*, *Boscia arabica*, and *Ziziphus spina-christii* (Miller and Morris, 1988; El-Sheikh, 2013; Patzelt, 2015; McCorriston et al., 2018). Taxa affiliated with this zone are considered more mesic for this region, as they have access to more rainfall annually and are nearer to permanent freshwater sources.

The plateau is a flat, high-elevation band that is mainly grassland (Poaceae) with isolated tree taxa such as *Senegalia* and shrubs (e.g., *Euphorbia* spp.; Miller and Morris, 1988; McCorriston et al., 2020). The Nejd lies furthest inland and is mainly desert, with isolated trees and shrubs that dot the cliff sides and dry wadi riverbeds. Notable taxa in this zone are frankincense trees (*Boswellia sacra*) and *Senegalia*, as well as herbs like *Cleome* and *Heliotropium* (Miller and Morris, 1988). *Cadaba heterotricha* is a shrub which is rare in this region today, but typically found in drier wadi beds in the Nejd (Miller and Morris, 1988; Abbas et al., 2010; McCorriston et al., 2018). Most taxa in the Njed, with the exception of those that grow surrounding freshwater springs in oases are considered xeric and exist in hyperarid conditions beyond the reach of the monsoon.

1.2 Leaf wax *n*-alkanes

n-Alkanes are long-chain hydrocarbons that are a component of plant leaf waxes (Chibnall et al., 1934; Killops and Killops, 2013). Those sourced from higher terrestrial plants show a strong odd over even preference for number of carbon atoms and tend to form longer chains (C25–C35) (Chibnall et al., 1934; Eglinton and Hamilton, 1963; Eglinton and Hamilton, 1967; Killops and Killops, 2013; Bush and McInerney, 2015). These biomarkers are insoluble in water and preserve well over long periods of time, and the isotopes of both carbon and hydrogen within these compounds record past changes in vegetation and rainfall, respectively (Pedentchouk et al., 2006; Eglinton and Logan, 1991; Peters et al., 2005; Sessions and Hayes, 2005; Sachse et al., 2012; Bush and McInerney, 2015). This makes *n*-alkanes a useful biomarker that can be extracted from geological materials for paleoecological analyses (Bush and McInerney, 2015; Eglinton and Eglinton, 2008).

Compound-specific $\delta^{13}C_{wax}$ is sensitive to the isotopic composition of atmospheric CO_2, the photosynthetic pathway of the plant (C3, C4, or CAM), as well as moisture availability (Ehleringer et al., 1997; Sage, 2004; Eglinton and Eglinton, 2008). In C3 plants, lower $\delta^{13}C_{wax}$ values, as for plant biomass, occur under higher humidity (Rao et al., 2017; Diefendorf et al., 2010). The C4 photosynthetic pathway is mostly found in grasses and sedges and evolved to limit water loss via transpiration, thus, these plants are better adapted to warmer and more arid climates (Ehleringer et al., 1997; Keeley and Rundel, 2003; Sage, 2004; Feakins et al., 2020). Crassulacean acid metabolism (CAM) is used in plants that conduct CO_2 fixation at night and is most predominant in succulents (Keeley and Rundel, 2003).

Lower $\delta^{13}C_{wax}$ values (avg. −36‰) are associated with C3 vegetation, while higher values (avg. −21.5‰) are associated with C4 plants (Castañeda et al., 2009; Rao et al., 2017). Fractionation of carbon isotopes occurs during plant uptake and fixation of atmospheric carbon (Farquhar et al., 1989; Diefendorf et al., 2010). The degree of fractionation can vary based on precipitation and other environmental conditions, as well as plant functional type (Farquhar et al., 1989; Diefendorf et al., 2010). Overall, however, $\delta^{13}C_{wax}$ values reflect the relative proportions of C3/C4 vegetation (Chikaraishi and Naraoka, 2007; Rao et al., 2017; Liu and An, 2020).

The hydrogen in *n*-alkanes is ultimately sourced from meteoric water, thus the isotopic composition is generally controlled by environmental factors such as latitude, humidity, and temperature (Dansgaard, 1964; Rozanski et al., 1993; Liu and Yang, 2008; Feakins et al., 2018; Polissar and Freeman, 2010). The amount effect summarizes the change in δD of precipitation (δD_p): as the amount of rainfall increases, the δD_p of precipitation decreases (Dansgaard, 1964). δD_p also decreases as an air mass moves inland or higher up in altitude, preferentially raining out isotopically heavy water and leaving behind isotopically light vapor (Dansgaard, 1964; Rozanski et al., 1993; Herrmann et al., 2017). Meteoric waters enter soils, where evaporation can impact the isotopic composition of this new isotopic pool, especially in arid ecosystems (Feakins and Sessions, 2010).

Plants take up water from the soil, which does not cause any fractionation, and use it to synthesize leaf wax *n*-alkanes (Sachse et al., 2012; Tipple et al., 2013). The biosynthesis of these compounds causes significant fractionation to the hydrogen isotopes, which varies between C3/C4/CAM plants as well as between plant habits (Sachse et al., 2012). Because of this, δD_{wax} values are often corrected using mixing-models which consider photosynthetic pathways and plant groups such as trees and herbs (Feakins, 2013). Transpiration of leaf waters can also impact resultant δD_{wax} values, such that the *n*-alkanes will record an enrichment in deuterium relative to meteoric waters (Feakins and Sessions, 2010; Kahmen et al., 2013). Additionally, biosynthesis of these lipid molecules causes significant isotopic fractionation, which varies taxonomically (Sachse et al., 2012; Feakins, 2013). Overall, less negative values of δD_{wax} indicate more arid conditions, making the δD_{wax} and $\delta^{13}C_{wax}$ records from *n*-alkanes complementary paleoenvironmental signals (Sachse et al., 2012; Rao et al., 2017). These compounds have been shown to preserve in rock hyrax middens over geologic timescales in South Africa and can be used to strengthen paleoecological studies in southern Arabia (Carr et al., 2010; Chase et al., 2012; Carr et al., 2016).

2 Methods

2.1 Rock hyrax middens

Rock hyraxes use communal latrines that result in indurated masses of hyraceum (a urinary product) and fecal material. This material traps pollen and other paleoenvironmental indicators and can preserve them for thousands of years (Scott and Cooremans, 1992; Scott and Woodborne, 2007; Carr et al., 2010; Chase et al., 2012; Carr et al., 2014; Ivory et al., 2021). The samples used in this study represent thin (<5 cm) accumulations, which we assume represent decades to ~100 years of deposition, based on investigations from Ivory et al. (2021) which obtained multiple radiocarbon ages from the same middens which were not significantly different. Radiocarbon dates obtain a single representative age. We interpret paleoenvironmental information from these samples as a "snapshot" of the landscape over ~101–102 years (Horisk et al., 2023). Approximately 100 g of material from 14 hyrax middens were disaggregated in 1 L of deionized water for pollen analysis as presented in Horisk et al. (2023). The rehydrated urine was sieved at 500 μm to remove fecal pellets and other macrobotanicals, and 10 fecal pellets from each sample were homogenized and radiocarbon dated at the University of Georgia Center for Applied Isotope Studies via Accelerated Mass Spectrometry (AMS) radiocarbon dating. Calibrated ages were obtained using the IntCal Northern Hemisphere Radiocarbon Age Calibration C (Reimer et al., 2020). A standard 40 mL of the liquid <500 μm fraction was then used to obtain pollen data. The archived portion of this rehydrated hyraceum (unfiltered) was employed to extract leaf wax *n*-alkanes as well as to conduct δD_{wax} and $\delta^{13}C_{wax}$ analyses. The use of the liquid fraction ensures the two datasets are directly comparable.

To obtain the Total Lipid Extract (TLE), 50 mL of the liquid fraction was frozen and then freeze-dried in ashed 500 mL beakers. Approximately 20 mL of a 2:1 azeotrope of Dichloromethane (DCM) to Methanol (MeOH) was added to the beaker and sonicated for 30 min, and the extracted TLE was pipetted into 50 mL vials. This process was repeated three times. A portion of the TLE (~8 mL) was archived before conducting further analysis. The TLE was separated into an acid and neutral fraction by adding water and salt through Bligh-Dyer separation, using the Wakeham and Pease (1992) protocol. Approximately 60 mL of TLE was added to a separatory funnel along with ~20 mL of 5% NaCl solution. The separatory funnel was inverted and degassed 5–7 times, and the bottom fraction was collected into an ashed flask. This process was repeated an additional two times to obtain the neutral fraction. To collect the acid fraction, the remaining 5% NaCl solution was acidified using HCl to reach a pH of ~2, then extracted three times using DCM.

The neutral fraction was separated into compound fractions via silica gel column chromatography. The column was constructed using a glass pipette and ashed silica gel and an ashed glass wool plug. The first fraction was eluted using hexane, and a second fraction was extracted using 2:1 DCM to MeOH. The hexane fraction (F1) was dried gently with N_2 in a FlexiVap, then 200 μL of hexane were quantitatively added to the vial prior to Gas Chromatography-Flame Ionization Detector (GC-FID) analysis. *n*-Alkane peaks were identified and quantified on the GC-FID using a 2 μL injection volume and a calibration curve with 5, 10, 25, and 50, and 100 ng/μL standards, and the response curve was generated after each batch of samples. The standard deviation of the peak areas for the standards ranged from 0.15 to 1.3 pA ∗ min, which is an error of approximately 7%.

The concentrations reported here are volumetric, since a liquid sample was used. However, we normalized abundance to a mass of organic material extracted, weighed some of the freeze-dried samples and conducted a unit conversion. These ranged from 0.20 to 1.8 μg/g of *n*-alkanes in relation to the mass of dried organic material. The middens analyzed by Carr et al. (2010) had average

n-alkane concentrations of 0.005–0.157 μg/g. One explanation for this discrepancy would be higher fecal pellet concentration in the middens of this study, and thus more leaf material from hyrax browsing. Moreover, if the yield was incomplete, sample amount would be underestimated. However, when middens were processed via sonication extraction in 9:1 DCM:MeOH and silica gel column separation alone (without a Bligh-Dyer separation), our *n*-alkane yields were much lower (<0.02 μg/g), suggesting that the addition of the Bligh-Dyer step to the methodology improves yields for midden samples with low concentrations.

Ten of these samples were shipped to the University of California Davis Stable Isotope Facility for $\delta^{13}C_{wax}$ analyses. The resulting dataset had a standard deviation of ±0.82‰ and an overall accuracy of ±0.29‰. We obtained δD_{wax} measurements on five samples at Penn State in the Deines Stable Isotope Laboratory. For each sample, 4 μL/100 was injected into the GC open split to a Finegan Delta Plus XP isotope-ratio mass spectrometer (IRMS). The A6 standard (A.Schimmelmann, Indiana University) was used, and the lowest peak area that produced reliable values was ~6 Vs. Due to this analytical constraint, only measurements above 6 Vs. were considered for analysis. The instrument δD_{wax} measurements were converted to VSMOW scale and analytical uncertainty was calculated using the methods of Polissar and D'Andrea (2014). This includes calculating standard deviation of replicate measurements ($n \geq 4$ for each sample), then propagating errors from measured and known values on the VSMOW scale (Polissar and D'Andrea, 2014). This uncertainty was estimated as the standard error of the mean and was between ± 4.1‰–6.2‰.

2.2 Modern herbarium specimens

Plant specimens from herbarium sheets collected in Dhofar in 2018 and housed in the Ohio State University Archeobotany Lab were sampled for geochemical analyses. For *n*-alkane analyses, 94–699 mg of leaf material was extracted using Accelerated Solvent Extraction (ASE), then separated into a hexane fraction and 1:1 DCM:MeOH fraction via the same silica gel column chromatography protocol used for the midden samples. The hexane fraction was evaporated using the FlexiVap, and 50 μL of hexane were quantitatively added to each sample for GC-FID analysis. A 2 μL injection was used and calibration standards of 5, 10, 25, 50, and 100 ng/μL were employed to create a calibration curve.

3 Results

3.1 Modern herbarium specimens

The *n*-alkanes from leaves from herbarium specimens were identified and quantified on the GC-FID, and values ranged from 0.72 to 380 ng/μL. In six samples, concentrations of the long-chain odd *n*-alkanes were too low and not identified by the instrument (labelled "n/a" in Table 1). The proportions of the C27, C29, and C31 + C33 *n*-alkanes in each sample were plotted in a histogram and on ternary diagrams (Figures 2, 3).

The histogram in Figure 2 illustrates that the C27 and C29 *n*-alkanes were highest in relative abundance in comparison to the combined abundances of C31 + C33 homologues from tree taxa (*Terminalia dhofarica*, *Salvadora persica*, *Boscia arabica*, *Ziziphus spina-christii*) on average (C27 = 21.0%, C29 = 29.5%, C31 + C33 = 37.5%). The C31 + C33 homologues were most abundant (C31 + C33 = 76.8%) among the herbaceous taxa (*Lasiurus scindicus* [Poaceae], *Cleome brachycarpa*, *Cenchrus ciliaris* [Poaceae], *Heliotropium fartakense*) compared to the other two homologues (C27 = 8.1%, C29 = 9.3%). Amongst the trees, *Ziziphus spina-christii* had a higher proportion of the C31 + C33 *n*-alkanes (70.0%) in comparison to all other taxa (8.9%–60.0%). The highest abundance of the C31 + C33 homologues was in the shrub *Cadaba heterotricha* (~99.5%).

In general, taxa with xeric affinities (*Cadaba heterotricha*, *Lasiurus scindicus*, *Cleome brachycarpa*, *Cenchrus ciliaris*, *Heliotropium fartakense*) had higher proportions of the C31 + C33 chains (>50%). Taxa with mesic affiliations (*Terminalia dhofarica*, *Salvadora persica*, *Boscia arabica*, *Ziziphus spina-christii*), except for *Ziziphus spina-christii*, were more abundant in the C27 and C29 chains (C27 + C29 > 50%).

3.2 Rock hyrax middens

The concentrations of *n*-alkanes from the hyrax middens ranged from 0.82 to 270 ng/μL (Table 2). One modern and five fossil samples had high enough concentrations of the C31 *n*-alkane to yield compound specific $\delta^{13}C_{wax}$ values. These values ranged −34.72 to −28.14‰. Peak areas of the C31 *n*-alkane ranged from 2.42 to 40.56 Vs. The average δD_{wax} values of the C31 *n*-alkane from one modern and three fossil middens ranged from −153.8 to −121.1‰ vs. VSMOW. Sample 103-2C (3,103 cal yr BP) did not yield any peaks above the analytical threshold, but samples 135-1, 146, 111-2 E, and 155-D (0, 706, 1,651, and 2,920 cal yr BP, respectively) yielded 2–4 replicates with a high enough peak area.

4 Discussion

4.1 Interpreting plant community change through *n*-alkane distributions

The proportions of the C27, C29, and C31 + C33 *n*-alkanes in the modern plant specimens largely reflect their plant habit, whether they are classified as herbs or trees/shrubs, which supports previous studies in other regions (Smith et al., 2007; Carr et al., 2014; Bush and McInerney, 2015). One notable exception, the shrub *Cadaba heterotricha*, had the highest proportion of C31 + C33 *n*-alkanes. This plant is found only in the drier wadis of Dhofar and has xerophyte characteristics such as trichomes (Miller and Morris, 1988). Xerophytic plants tend to produce a higher concentration of *n*-alkanes and are typically abundant in the C31 chain length (Boom et al., 2014; Carr et al., 2014). The taxon *Ziziphus spina-christii* had the lowest relative abundances of the C27 and C29 chains in comparison to other trees. This plant typically has an arboreal habit and is distributed mainly throughout the monsoon-affected (mesic) areas of Dhofar (Miller and Morris, 1988). However, it can also grow as a shrub, and like *C. heterotricha* this shrub habit may

10.3389/feart.2024.1441323

TABLE 1 *n*-Alkane chain length concentations for herbarium plant samples.

Id	Species	Family	Mass (mg)	C27 (ng/g)	C29 (ng/g)	C31 (ng/g)	C33 (ng/g)
1	*Croton oblongifolius*	Euphorbiaceae	301	n/a	n/a	n/a	n/a
2	*Pulicaria glutinosa*	Asteraceae	201	n/a	n/a	n/a	n/a
3	*Cadaba heterotricha*	Capparaceae	434	5.20	11.00	180.00	240.00
4	*Euphorbia granulata*	Euphorbiaceae	84	15.00	30.00	100.00	20.00
5	*Salsola rubescens*	Amaranthaceae	421	1.90	2.10	0.52	0.12
6	*Terminalia dhofarica*	Combretaceae	94	20.00	32.00	12.00	0.79
7	*Heliotropium fartakense*	Boraginaceae	384	3.00	5.00	24.00	2.30
8	*Salvadora persica*	Salvadoraceae	404	2.20	3.00	2.40	0.30
9	*Cleome* sp.	Capparaceae	102	2.50	18.00	21.00	7.80
10	*Pluchea dioscoridis*	Asteraceae	423	n/a	n/a	n/a	n/a
11	*Halothamnus bottae*	Amaranthaceae	313	n/a	n/a	n/a	n/a
12	*Cadaba farinosa*	Capparaceae	201	1.30	0.72	n/a	n/a
13	*Cleome brachycarpa*	Capparaceae	239	13.00	27.00	270.00	330.00
14	*Ziziphus spina-christi*	Rhamnaceae	284	7.30	21.00	48.00	8.00
15	*Fiscus cordata*	Moraceae	699	n/a	n/a	n/a	n/a
16	*Boscia arabica*	Capparaceae	272	27.00	79.00	68.00	3.10
17	*Cocculus pendulus*	Menispermiaceae	100	n/a	n/a	n/a	n/a
18	*Indigofera coerulea*	Fabaceae	271	1.10	1.20	0.79	0.11
19	*Lasiurus scindicus*	Poaceae	223	3.30	n/a	5.90	14.00
20	*Cenchrus ciliaris*	Poaceae	106	18.00	45.00	n/a	48.00

explain the higher relative abundances of the longer chains (Miller and Morris, 1988).

When modern plant specimens were distinguished by their ecological affinity, whether they are generally associated with more mesic (*Terminalia dhofarica*, *Salvadora persica*, *Boscia arabica*, *Ziziphus spina-christii*) or xeric habitats (*Cadaba heterotricha*, *Lasiurus scindicus*, *Cleome brachycarpa*, *Cenchrus ciliaris*, *Heliotropium fartakense*) (Figure 3). In Dhofar, xeric plants were also more abundant in C31 + C33 homologues (79.5% of total C-27, 29, 32, and 33 homologues). Plants that were affiliated with more mesic environments had a higher proportion of C27 and C29 chains (25.1% and 30.8%; Miller and Morris, 1988). These results indicate that in Dhofar, both plant habit and ecology impact the distribution of *n*-alkanes, which would then be preserved in paleoecological archives and can aid in interpretations of vegetation change (Smith et al., 2007; Boom et al., 2014; Carr et al., 2014).

4.2 Applications of leaf wax isotopes for hyrax middens

While previous studies have extracted high enough concentrations of *n*-alkanes from hyrax middens for compound specific carbon isotope analyses, there is yet no published δD_{wax} data from fossil hyrax middens (Carr et al., 2010; Chase et al., 2012; Boom et al., 2014; Carr et al., 2014; Carr et al., 2016). The method used for this study has proven to yield higher concentrations of *n*-alkanes, and thus reproducible δD_{wax} values. Published *n*-alkane concentrations from hyrax middens are as low as 0.0002 μg/g (Carr et al., 2010). In comparison, ocean cores and terrestrial sediments range from 0.4 to 1.3 μg/g (Carr et al., 2010). Compound specific hydrogen isotope values have been successfully measured on samples with low concentrations of terrestrial *n*-alkanes, but these were two orders of magnitude larger than the previous midden studies (Carr et al., 2014; Aichner et al., 2015).

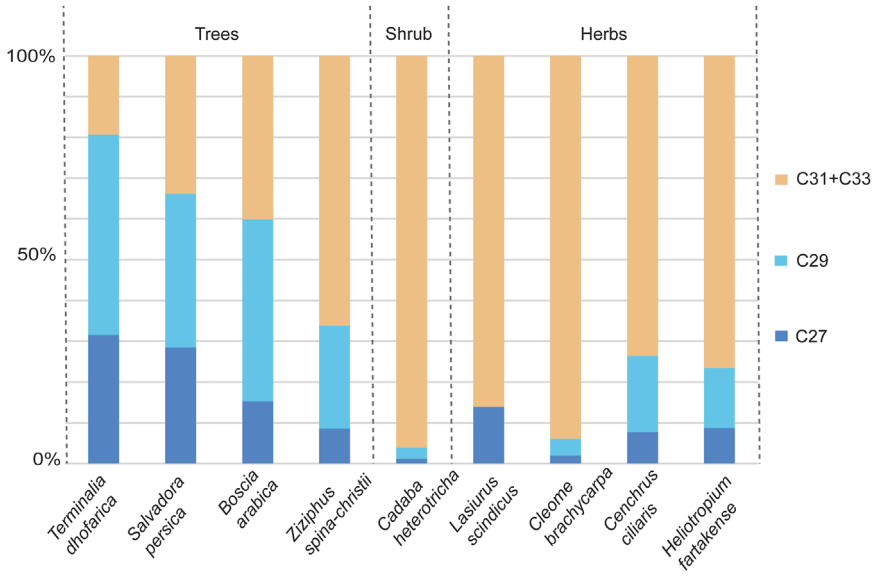

FIGURE 2
Proportions of the C27, C29, and C31 + C33 *n*-alkanes in plant herbarium specimens. The C27 and C29 compounds are generally associated with trees, and the C31 + C33 with herbs and grasses. From left to right are the Trees: *Terminalia dhofarica, Salvadora persica, Boscia arabica, Ziziphus spina-christii*; Shrub: *Cadaba heterotricha*; Herbs: *Cleome, Cenchrus ciliaria, Euphorbia granulata, Heliotropium fartakense, Cleome brachycarpa*.

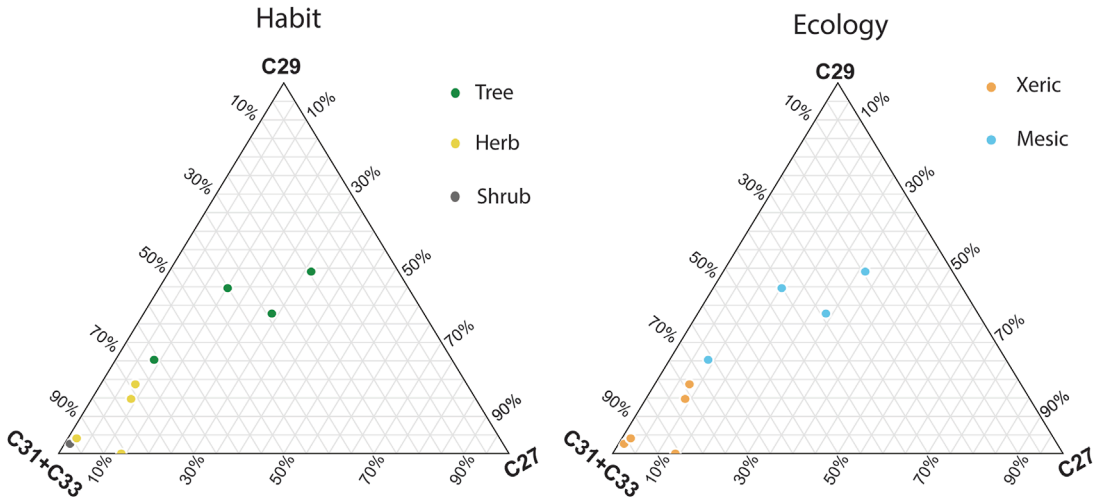

FIGURE 3
Ternary plots showing the proportions of the C27, C29, and C31 + C33 *n*-alkanes in plant herbarium specimens. The left panel is color-coded by plant habit (tree, herb, or shrub) and the right panel is color-coded based on ecological affinity in the region (more mesic or xeric).

4.3 Paleohydrology and vegetation change in the late Holocene

The *n*-alkane chain length proportions from fossil hyrax middens had some variability, but generally remained dominated by C31 + C33 chain lengths (Figure 4; ~60%). Samples with higher proportions of the shorter chain lengths (C27 and C29) often correlate to high percentages of tree pollen. This revealed that overall, little change occurred in the predominant vegetation over this period from ~4 cal yr BP to modern, and that the plant community remained dominated by herbaceous plants. Further, other indications of changes in the proportion of vegetation types, including bulk $\delta^{13}C$, and $\delta^{13}C_{wax}$ values, do not indicate a notable shift. Taken together, this suggests that the overall structure of the ecosystem in relation to C3 and C4 plants and woody versus herbaceous taxa, did not significantly change. In contrast, the pollen data produced from the same middens implied considerable turnover in the plant community, and the composition of the pollen flora in each pollen zone was demonstrated to be statistically different through time (Horisk et al., 2023). In particular, the pollen

TABLE 2 *n*-Alkane chain length concentrations and stable isotope results for the hyrax midden samples. Bulk $\delta^{13}C$ values come from (Horisk et al., 2023).

ID	Latitude	Longitude	Age (cal yr BP)	Bulk $\delta^{13}C$ (‰)	δD_{wax} C31 (‰)	$\delta^{13}C_{wax}$ C31 (‰)	C27 (ng/μL)	C29 (ng/μL)	C31 (ng/μL)	C33 (ng/μL)
135–1	17°14.618′N	53°53.380′E	0	−27.53	−125.8	−32.4	16.00	53.00	110.00	47.00
48-1B	17°25.431′N	54°29.385′E	0	−28.12		−34.7	0.84	2.20	5.00	0.37
108-1b	17°23.123′N	54°29.767′E	109	−25.65		−32.6	8.80	14.00	16.00	4.40
107-2b	17°23.110′N	54°29.755′E	114	−25.96			4.30	6.90	13.00	1.50
146	17°23.523′N	54°31.010′E	706	−24.86			16.00	49.00	150.00	47.00
155-2C	17°24.513′N	54°30.555′E	1,403	−25.49			7.10	9.00	13.00	3.00
147–1	17°23.331′N	54°30.724′E	1,466	−26.32			13.00	29.00	78.00	19.00
151	17°23.305′N	54°30.724′E	1,574	−26.2		−28.1	0.82	1.10	1.40	1.40
145–4	17°23.733′N	54°30.996′E	1,638	−25.69			9.00	13.00	25.00	8.60
111-2 E	17°23.142′N	54°29.869′E	1,651	−26.94	−153.8	−31.8	6.60	14.00	35.00	14.00
155-D	17°24.513′N	54°30.555′E	2,920	−26.87	−144.7		31.00	83.00	270.00	130.00
103-2c	17°25.338′N	54°29.861′E	3,103	−24.13	−121.0		7.70	16.00	34.00	15.00
149-2	17°23.298′N	54°30.711′E	3,233	−25.82		−31.9	2.30	4.10	5.70	5.50
155-F	17°24.513′N	54°30.555′E	4,038	−25.85		−31.1	2.00	4.20	10.00	4.80

record shows that from ~4 to 3.1 ka, there were higher abundances of arboreal vegetation associated with escarpment woodlands and edaphically wetter locations like *Terminalia*, *Maytenus*, and *Boscia* (Horisk et al., 2023). After ~1.6 ka, there was a large shift to predominantly herbaceous taxa, such as Poaceae and *Heliotropium* (Horisk et al., 2023).

Although the results of the pollen, n-alkane abundance patterns, and δ13C data from the same middens seem to disagree, we suggest that pollen and n-alkanes instead provide separate pieces of information about regional vegetation that represent different spatial and taxonomic scales. The pollen from the middens may represent a more regional signal, capturing vegetation changes on the plateau, while the n-alkanes more closely represent the local plant community. This suggests pollen deposition into the middens is primarily aeolian and represents a larger catchment area. This is supported by other midden studies which show their pollen spectra closely align with surface soil pollen spectra, and thus pollen is primarily deposited through environmental processes, such as aeolian deposition (Scott and Cooremans, 1992; Scott and Woodborne, 2007). In contrast, the bulk of the n-alkanes may have largely been deposited through dietary consumption of plant materials, which is supported by the previous study of Carr et al. (2010). Thus, the environmental signal would be geographically restricted to the smaller foraging range of the hyrax and represent local, rather than more regional, vegetation.

While the alkane data provide a broad picture of local abundances of xeric vegetation structure, they do not provide detailed information about the taxonomy of plants more regionally as revealed by pollen data. The significant changes in the pollen composition over this interval suggest there was turnover in the ecosystem composition over the late Holocene. At a course resolution, the vegetation structure, in terms of the distribution of herbaceous versus arboreal plants, did not shift significantly in the Nejd over the last 4,000 years. However, it is likely that there was a higher density of mesic, arboreal vegetation on the plateau and escarpment from ~4 to 3 ka.

Further, we suggest that turnover in plant communities over the late Holocene in the Nejd was driven by variability in rainfall across the late Holocene, as revealed by the high-resolution oxygen isotope record (Fleitmann et al., 2007). Although only two samples were available prior to 1.6 ka, δD_{wax} (−144.7‰ to −153.8‰) values were lower in comparison to the more recent values, indicating relatively higher moisture availability earlier in the record (Figure 5; Sachse et al., 2012). Sedimentological data and pollen evidence from Khor Rori estuary demonstrated increased surface water flow at ~1.6 ka (Hoorn and Cremaschi, 2004), indicating a wetter pulse around ~1.6 ka punctuated the overall drying trend across the late Holocene (Hoorn and Cremaschi, 2004; Fleitmann et al., 2007). The δD_{wax} data from this time which indicate higher moisture availability are in line with this previously established hydrological

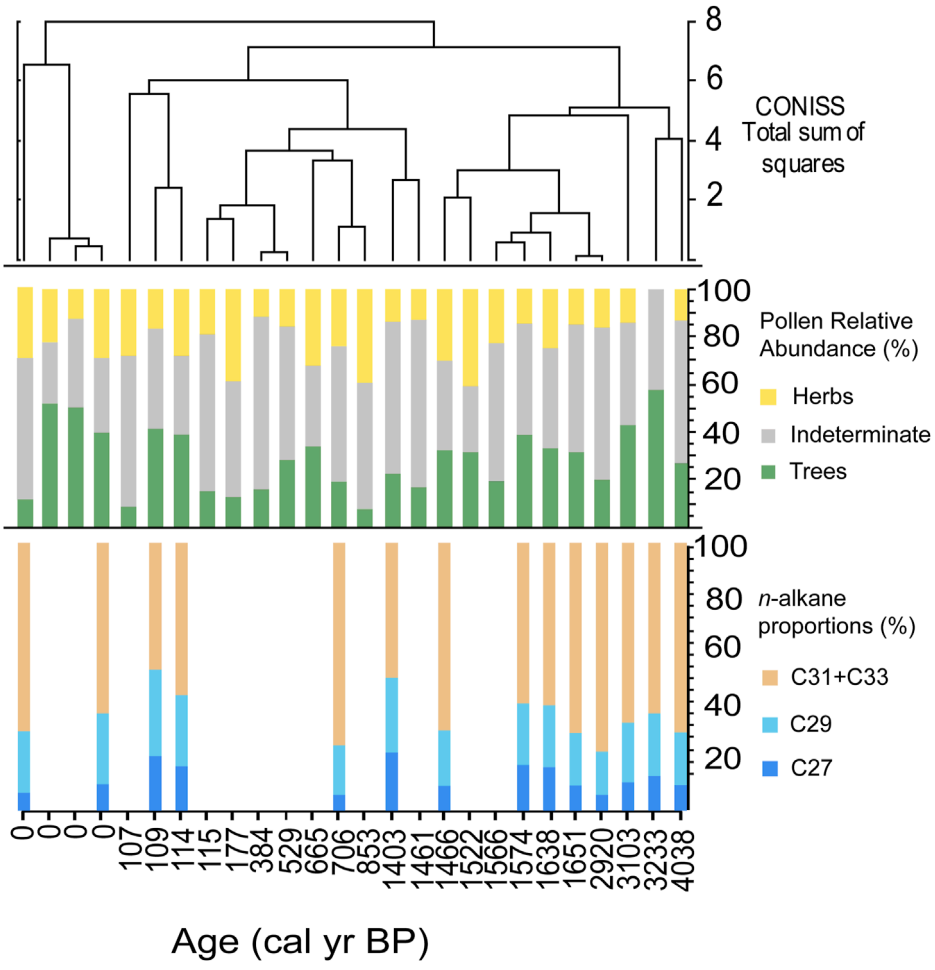

FIGURE 4
From top to bottom: CONISS cluster analysis (Grimm, 1987) of the relative abundances of the pollen in each sample; the relative abundances of Tree, Herb, and Indeterminate pollen habits; proportions of *n*-alkane homologues in each sample.

record. In contrast, the two more recent δD_{wax} samples at 706 and 0 cal yr BP were both higher than the older samples by ~20‰–30‰, which suggests less moisture availability and modern-like conditions by ~700 years ago.

The $\delta^{13}C_{wax}$ results suggest an admixture of C4 grasses and C3 woody plants, with a predominance of *n*-alkane homologues associated with C4 vegetation from ~4 to 3 kyr. The $\delta^{13}C_{wax}$ values at ~1.6 kyr were more variable, with one lower value (111-2E; −31.78‰) and one higher value (151; −28.14‰). The variability between these two samples may be a product of some temporal and spatial heterogeneity between the two samples, but on average represent a mixed C3/C4 cover (Chikaraishi and Naraoka, 2007; Rao et al., 2017; Liu and An, 2020). The sub-modern sample (108-1b, 109 cal yr BP) has a similar value to the older samples, and one modern sample (48-1b) shows a 2‰ depletion in line with the Suess Effect (Keeling, 1979; Feakins et al., 2015).

Given the $\delta^{13}C_{wax}$ results, we assume an average fractionation factor (ε) to make a tentative comparison to modern meteoric δD values. Feakins (2013) report an average ε value of −150‰ in C3 monocots and −134‰ in C4 monocots. Due to the mix of this vegetation in our record, we apply a simple average of these two values for an ε of −142‰. These values were plotted in comparison to modern measurements on both meteoric and groundwater in Dhofar (Figure 6; Al-Mashaikhi et al., 2012; Strauch et al., 2014; Friesen et al., 2018). These show that samples dated to 2,920 and 1,651 cal yr BP have lower values of the δD_{wax} that are similar to modern Nejd groundwater (approximately −40 to −20‰). This could indicate groundwater recharge in the Nejd at this time, or perhaps more input from cyclone events. Modern meteoric water from cyclones is far more depleted in hydrogen and oxygen than monsoon precipitation (δD values −80 to −50‰; Al-Mashaikhi et al., 2012; Strauch et al., 2014; Friesen et al., 2018). These events originate in the Arabian Sea and occur generally once every 3 years, with a severe storm once in every five (Kwarteng et al., 2009). Cyclonic events cause increased runoff, which is indicated by sedimentological records from coastal estuaries at ~1.6 kyr (Hoorn and Cremaschi, 2004).

The younger samples (706 cal yr BP and modern) were in the range of modern monsoon rainfall values and runoff (approx. −5–20‰). Thus, higher values in the younger samples could indicate a change in water source to runoff from monsoon rainfall occurring on the escarpment and/or increased evapotranspiration.

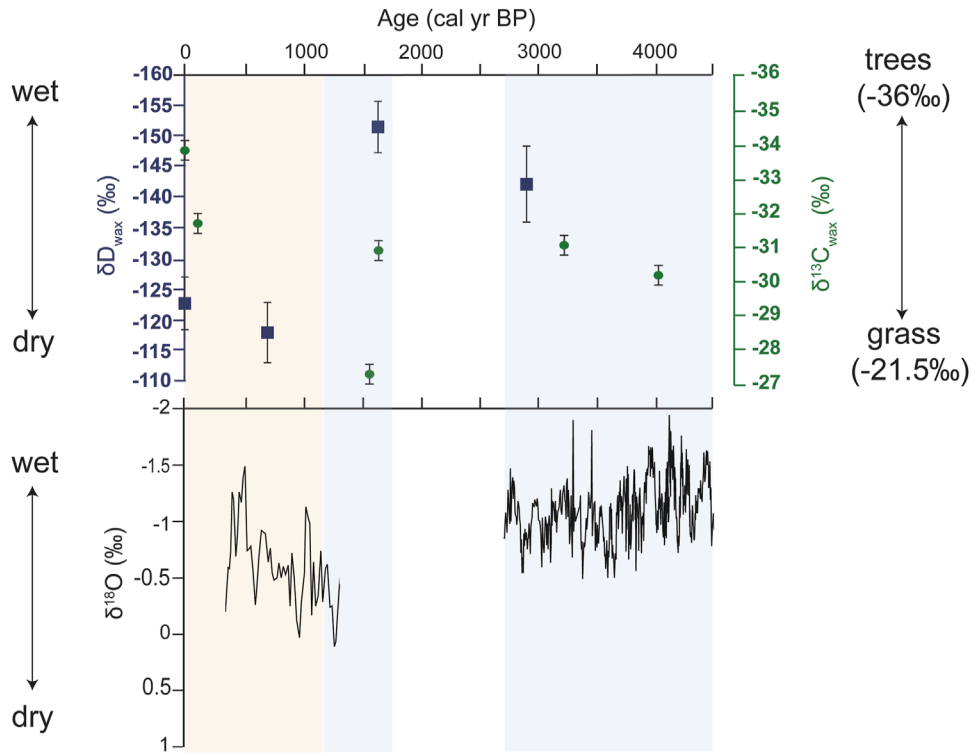

FIGURE 5
Top panel: δD_{wax} (blue) and $\delta^{13}C_{wax}$ data (green) plotted against midden sample age (cal yrs BP). Bottom panel: $\delta^{18}O$ data replotted from the Qunf cave speleothem record of Fleitmann et al., 2007. Blue bars represent periods where local and regional records indicate it is relatively wetter, compared to yellow bar which is a time frame that is generally accepted to be the driest time.

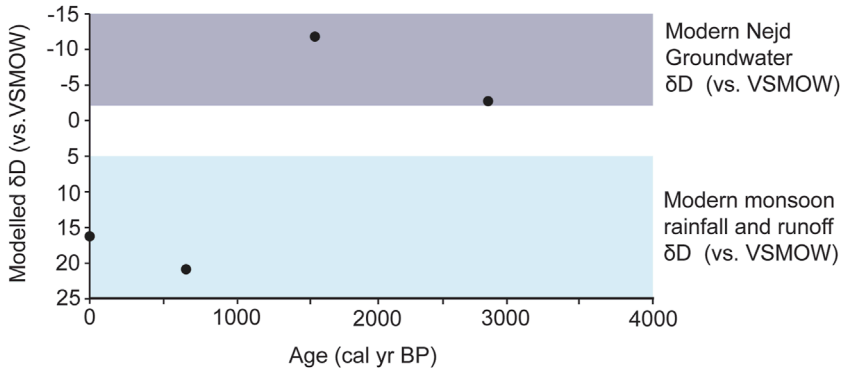

FIGURE 6
δD_{wax} data with applied ε value based on average of the C3 and C4 plant ε values described in the literature. Purple bar represents range of isotopic values from modern Nejd groundwater and the blue from modern monsoon rainfall and runoff, as presented by Strauch et al. (2014) and Friesen et al. (2018).

In comparison to cyclones, winds from the monsoon transport moisture from the southern Indian Ocean (Fleitmann et al., 2007). Due to this larger transport distance, the moisture that is released over Dhofar has a higher hydrogen isotope composition due to the latitudinal effect (Dansgaard, 1964; Fleitmann et al., 2007).

The speleothem record from Qunf Cave indicates decreasing rainfall across the Holocene through gradual $\delta^{18}O$ enrichment (Fleitmann et al., 2007). Sedimentological data from Khor rori estuary, as well as the δD_{wax} values suggest a wetter pulse. This may be indicative of groundwater recharge or an uptick in cyclonic events at ~1.6 ka. All three records independently indicate it was dryer by ~1 kyr–~700 yr in Dhofar, and particularly locally in the Nejd (Smith and Freeman, 2006; Fleitmann et al., 2007; Sachse et al., 2012). This information suggests that despite an overall drying trend across the Holocene, we capture shorter-term variability in rainfall previously demonstrated by Hoorn and Cremaschi (2004).

While the pollen habits (trees, indeterminate, herbs) suggested large changes in community composition over the late Holocene, the geochemical data indicate there was little to no changes in local structure, and that arid and semi-arid desert scrub taxa dominated over the entire interval. This implies the Nejd vegetation communities may be resistant to large-scale changes in intensity and variability of hydroclimate and aridity, which global climate models predict will become more severe in the next century (Dahinden et al., 2017). However, substitutions within the major plant habit groups may result in the loss of species that are used as fodder for domesticate animals (e.g. *Terminalia*, *Salvadora persica*) or are economically important (e.g., Frankincense) across the vegetation zones, which could drastically impact economic resources, foodways, and timber (Asner et al., 2004; El-Mahi, 2011; Ball and Tzanopoulos, 2020). Overgrazing and other human activity could potentially intensify this, thus mitigating these impacts should be a focus of conservation efforts.

Finally, Rock hyrax middens are an invaluable resource for understanding dryland ecosystem dynamics through time. The methods used to extract leaf wax n-alkanes and obtain compound-specific isotopes from hyrax middens in this study can be used to reconstruct paleoenvironmental changes in dryland regions where traditional archives, such as lake sediments, are unavailable. Rock hyraxes are widely distributed in Africa and Arabia (Sale, 1966), and other studies have used pollen, stable isotopes, and n-alkanes to conduct paleoenvironmental studies in South Africa (Scott and Cooremans, 1992; Scott and Woodborne, 2007; Carr et al., 2010; Chase et al., 2012; Carr et al., 2016). However, the δD_{wax} data represent the first of its kind generated from rock hyrax middens, and the geochemical techniques employed can be used to obtain additional local paleohydrological information in Oman and elsewhere on the African continent.

5 Conclusion

Dryland ecosystems are essential to nearly half of the Earth's population but are also the most at risk under changing climate conditions (Asner et al., 2004; Maestre et al., 2016). Global anthropogenic climate change is accelerating, and paleoecological records allow us to determine long-term patterns in changing climate and vegetation response. These can help scientists constrain future predictions of climate change impacts (Asner et al., 2004; Maestre et al., 2016; Dahinden et al., 2017). Rock hyrax middens have proven a powerful archive of both pollen and geochemical indicators, such as n-alkanes, δD_{wax}, and $\delta^{13}C_{wax}$, for paleoecological studies in arid regions (Chase et al., 2012; Carr et al., 2016). In Dhofar, a more complete picture of vegetation changes over the late Holocene and a link to changing hydroclimate was revealed by plant biomarkers and stable isotope records derived from middens.

δD_{wax} data support that over the course of regional drying, driven by Indian Monsoon dynamics, there may have been a shorter wet period at ~1.6 ka, as revealed by sedimentological data from a coastal estuary (Fleitmann et al., 2004; Hoorn and Cremaschi, 2004; Fleitmann et al., 2007). The leaf wax *n*-alkane distributions and $\delta^{13}C_{wax}$ values, in comparison with the pollen record, indicated that these hydrological changes drove changes in the composition of the local vegetation, but not the overall structure of the plant communities. This suggests resilience of dryland vegetation to state-shifts under increasing aridity, which global climate models predict will be amplified by climate change (Dahinden et al., 2017). More work is necessary to fully constrain local paleohydrological change in this region, which can be achieved through the previously outlined midden processing methods that yielded reproducible δD_{wax} data.

Data availability statement

The original contributions presented in the study are included in the article/supplementary material, further inquiries can be directed to the corresponding author.

Author contributions

KH: Conceptualization, Data curation, Funding acquisition, Investigation, Methodology, Visualization, Writing–original draft, Writing–review and editing. SI: Funding acquisition, Resources, Supervision, Writing–review and editing. KF: Conceptualization, Methodology, Project administration, Resources, Supervision, Validation, Writing–review and editing. AB: Conceptualization, Investigation, Methodology, Validation, Writing–review and editing. JM: Data curation, Funding acquisition, Project administration, Writing–review and editing. AA: Data curation, Resources, Writing–review and editing. RA: Conceptualization, Funding acquisition, Methodology, Writing–review and editing, AA-K: Conceptualization, Investigation, Project administration, Resources, Writing–review and editing.

Funding

The author(s) declare that financial support was received for the research, authorship, and/or publication of this article. Funding for this project was provided by NSF-CNH (1617185). Additional funding was earned through the Elsevier Organic Geochemistry Research Award and the Marilyn L. Fogel Award in Biogeosciences (Penn State Earth and Environmental Systems Institute).

Acknowledgments

The authors would like to thank the Oman Ministry of Heritage and Tourism under His Majesty Sultan Haitham Bin Tariq Al Said for their collaboration and hospitality while in the field, especially Ali Al Mehri. We would also like to express our gratitude to the Oman Botanic Garden, including AnA, Annette Patzelt, and Darach Lupton for their field surveying and collection of modern plant specimens used in this study. Special thanks to the entire Ancient

Socioecological Systems of Oman (ASOM) team for their invaluable input and constant support.

Conflict of interest

The authors declare that the research was conducted in the absence of any commercial or financial relationships that could be construed as a potential conflict of interest.

Publisher's note

References

Abbas, H., Qaiser, M., and Alam, J. (2010). Conservation status of *Cadaba heterotricha* Stocks (Capparaceae): an endangered species in Pakistan. *Pak. J. Bot.* 42 (1), 35–46.

Afuye, G. A., Kalumba, A. M., and Orimoloye, I. R. (2021). Characterisation of vegetation response to climate change: a review. *Sustainability* 13 (13), 7265. doi:10.3390/su13137265

Aichner, B., Feakins, S. J., Lee, J. E., Herzschuh, U., and Liu, X. (2015). High-resolution leaf wax carbon and hydrogen isotopic record of the late Holocene paleoclimate in arid Central Asia. *Clim. Past* 11 (4), 619–633. doi:10.5194/cp-11-619-2015

Al-Mashaikhi, K., Oswald, S., Attinger, S., Büchel, G., Knöller, K., and Strauch, G. (2012). Evaluation of groundwater dynamics and quality in the Najd aquifers located in the Sultanate of Oman. *Environ. Earth Sci.* 66 (4), 1195–1211. doi:10.1007/s12665-011-1331-2

Asner, G. P., Elmore, A. J., Olander, L. P., Martin, R. E., and Harris, A. T. (2004). Grazing systems, ecosystem responses, and global change. *Annu. Rev. Environ. Resour.* 29 (1), 261–299. doi:10.1146/annurev.energy.29.062403.102142

Ball, L., and Tzanopoulos, J. (2020). Livestock browsing affects the species composition and structure of cloud forest in the Dhofar Mountains of Oman. *Appl. Veg. Sci.* 23 (3), 363–376. doi:10.1111/avsc.12493

Bellini, C., Ciani, F., Pignotti, L., Baldini, R. M., Gonnelli, T., and Mariotti Lippi, M. (2022). Modern pollen analysis in the estuary habitats along the coast of dhofar (sultanate of Oman). *Sustainability* 14 (17), 11038. doi:10.3390/su141711038

Böll, A., Lückge, A., Munz, P., Forke, S., Schulz, H., Ramaswamy, V., et al. (2014). Late Holocene primary productivity and sea surface temperature variations in the northeastern Arabian Sea: implications for winter monsoon variability: late Holocene winter monsoon variations. *Paleoceanography* 29 (8), 778–794. doi:10.1002/2013PA002579

Boom, A., Carr, A. S., Chase, B. M., Grimes, H. L., and Meadows, M. E. (2014). Leaf wax n-alkanes and δ13C values of CAM plants from arid southwest Africa. *Org. Geochem.* 67, 99–102. doi:10.1016/j.orggeochem.2013.12.005

Bush, R. T., and McInerney, F. A. (2015). Influence of temperature and C 4 abundance on n -alkane chain length distributions across the central USA. *Org. Geochem.* 79, 65–73. doi:10.1016/j.orggeochem.2014.12.003

Carr, A. S., Boom, A., and Chase, B. M. (2010). The potential of plant biomarker evidence derived from rock hyrax middens as an indicator of palaeoenvironmental change. *Palaeogeogr. Palaeoclimatol. Palaeoecol.* 285 (3–4), 321–330. doi:10.1016/j.palaeo.2009.11.029

Carr, A. S., Boom, A., Grimes, H. L., Chase, B. M., Meadows, M. E., and Harris, A. (2014). Leaf wax n-alkane distributions in arid zone South African flora: environmental controls, chemotaxonomy and palaeoecological implications. *Org. Geochem.* 67, 72–84. doi:10.1016/j.orggeochem.2013.12.004

Carr, A. S., Chase, B. M., Boom, A., and Medina-Sanchez, J. (2016). Stable isotope analyses of rock hyrax faecal pellets, hyraceum and associated vegetation in southern Africa: implications for dietary ecology and palaeoenvironmental reconstructions. *J. Arid Environ.* 134, 33–48. doi:10.1016/j.jaridenv.2016.06.013

Castañeda, I. S., Werne, J. P., Johnson, T. C., and Filley, T. R. (2009). Late Quaternary vegetation history of southeast Africa: the molecular isotopic record from Lake Malawi. *Palaeogeogr. Palaeoclimatol. Palaeoecol.* 275 (1–4), 100–112. doi:10.1016/j.palaeo.2009.02.008

Chase, B. M., Scott, L., Meadows, M. E., Gil-Romera, G., Boom, A., Carr, A. S., et al. (2012). Rock hyrax middens: a palaeoenvironmental archive for southern African drylands. *Quat. Sci. Rev.* 56, 107–125. doi:10.1016/j.quascirev.2012.08.018

Chibnall, A. C., Piper, S. H., Pollard, A., Williams, E. F., and Sahai, P. N. (1934). The constitution of the primary alcohols, fatty acids and paraffins present in plant and insect waxes. *Biochem. J.* 28 (6), 2189–2208. doi:10.1042/bj0282189

Chikaraishi, Y., and Naraoka, H. (2007). Δ13C and δD relationships among three n-alkyl compound classes (n-alkanoic acid, n-alkane and n-alkanol) of terrestrial higher plants. *Org. Geochem.* 38 (2), 198–215. doi:10.1016/j.orggeochem.2006.10.003

Dahinden, F., Fischer, E. M., and Knutti, R. (2017). Future local climate unlike currently observed anywhere. *Environ. Res. Lett.* 12 (8), 084004. doi:10.1088/1748-9326/aa75d7

Dansgaard, W. (1964). Stable isotopes in precipitation. *tellus* 16 (4), 436–468. doi:10.3402/tellusa.v16i4.8993

Diefendorf, A. F., Mueller, K. E., Wing, S. L., Koch, P. L., and Freeman, K. H. (2010). Global patterns in leaf ^{13} C discrimination and implications for studies of past and future climate. *Proc. Natl. Acad. Sci.* 107 (13), 5738–5743. doi:10.1073/pnas.0910513107

Dietl, G. P., Kidwell, S. M., Brenner, M., Burney, D. A., Flessa, K. W., Jackson, S. T., et al. (2014). Conservation paleobiology: leveraging knowledge of the past to inform conservation and restoration. *Annu. Rev. Earth Planet. Sci.* 43, 79–103. doi:10.1146/annurev-earth-040610-133349

Eglinton, G., and Hamilton, R. J. (1963). The distribution of alkanes. *Chem. plant Taxon.* 187 (217), 50012–50019. doi:10.1126/science.156.3780.1322

Eglinton, G., and Hamilton, R. J. (1967). Leaf epicuticular waxes. *Am. Assoc. Adv. Sci.* 156 (3780), 1322–1335. doi:10.1126/science.156.3780.1322

Eglinton, G., and Logan, G. A. (1991). Molecular preservation. *Philosophical Trans. R. Soc. Lond. Ser. B Biol. Sci.* 333 (1268), 315–327. doi:10.1098/rstb.1991.0081

Eglinton, T. I., and Eglinton, G. (2008). Molecular proxies for paleoclimatology. *Earth Planet. Sci. Lett.* 275 (1-2), 1–16. doi:10.1016/j.epsl.2008.07.012

Ehleringer, J. R., Cerling, T. E., and Helliker, B. R. (1997). C 4 photosynthesis, atmospheric CO 2, and climate. *Oecologia* 112 (3), 285–299. doi:10.1007/s004420050311

El-Mahi, A. T. (2011). Old ways in a changing space: the issue of camel pastoralism in dhofar. *J. Agric. Mar. Sci. [JAMS]* 16, 51. doi:10.24200/jams.vol16iss0pp51-64

El-Sheikh, M. A. (2013). Population structure of woody plants in the arid cloud forests of Dhofar, southern Oman. *Acta Bot. Croat.* 72 (1), 97–111. doi:10.2478/v10184-012-0008-6

Farquhar, G. D., Ehleringer, J. R., and Hubick, K. T. (1989). Carbon isotope discrimination and photosynthesis. *Annu. Rev. Plant Physiology Plant Mol. Biol.* 40 (1), 503–537. doi:10.1146/annurev.pp.40.060189.002443

Feakins, S. J. (2013). Pollen-corrected leaf wax D/H reconstructions of northeast African hydrological changes during the late Miocene. *Palaeogeogr. Palaeoclimatol. Palaeoecol.* 374, 62–71. doi:10.1016/j.palaeo.2013.01.004

Feakins, S. J., Liddy, H. M., Tauxe, L., Galy, V., Feng, X., Tierney, J. E., et al. (2020). Miocene C $_4$ grassland expansion as recorded by the indus fan. *Paleoceanogr. Paleoclimatology* 35 (6). doi:10.1029/2020PA003856

Feakins, S. J., and Sessions, A. L. (2010). Controls on the D/H ratios of plant leaf waxes in an arid ecosystem. *Geochimica Cosmochimica Acta* 74 (7), 2128–2141. doi:10.1016/j.gca.2010.01.016

Feakins, S. J., Wu, M. S., Ponton, C., Galy, V., and West, A. J. (2018). Dual isotope evidence for sedimentary integration of plant wax biomarkers across an Andes-Amazon elevation transect. *Geochimica Cosmochimica Acta* 242, 64–81. doi:10.1016/j.gca.2018.09.007

Fleitmann, D., Burns, S. J., Mangini, A., Mudelsee, M., Kramers, J., Villa, I., et al. (2007). Holocene ITCZ and Indian monsoon dynamics recorded in stalagmites from Oman and Yemen (Socotra). *Quat. Sci. Rev.* 26 (1–2), 170–188. doi:10.1016/j.quascirev.2006.04.012

Fleitmann, D., Burns, S. J., Neff, U., Mudelsee, M., Mangini, A., and Matter, A. (2004). Palaeoclimatic interpretation of high-resolution oxygen isotope profiles derived from annually laminated speleothems from Southern Oman. *Quat. Sci. Rev.* 23 (7–8), 935–945. doi:10.1016/j.quascirev.2003.06.019

Friesen, J., Zink, M., Bawain, A., and Müller, T. (2018). Hydrometeorology of the Dhofar cloud forest and its implications for groundwater recharge. *J. Hydrology Regional Stud.* 16, 54–66. doi:10.1016/j.ejrh.2018.03.002

Ghazanfar, S. A. (1999). Coastal vegetation of Oman. *Estuar. Coast. Shelf Sci.* 49, 21–27. doi:10.1016/S0272-7714(99)80004-3

Grimm, E. C. (1987). CONISS: a FORTRAN 77 program for stratigraphically constrained cluster analysis by the method of incremental sum of squares. *Comput. and Geosciences* 13 (1), 13–35. doi:10.1016/0098-3004(87)90022-7

Herrmann, N., Boom, A., Carr, A. S., Chase, B. M., West, A. G., Zabel, M., et al. (2017). Hydrogen isotope fractionation of leaf wax n-alkanes in southern African soils. *Org. Geochem.* 109, 1–13. doi:10.1016/j.orggeochem.2017.03.008

Hildebrandt, A., Al Aufi, M., Amerjeed, M., Shammas, M., and Eltahir, E. A. B. (2007). Ecohydrology of a seasonal cloud forest in Dhofar: 1. Field experiment. *Water Resour. Res.* 43 (10). doi:10.1029/2006WR005261

Hoorn, C., and Cremaschi, M. (2004). Late Holocene palaeoenvironmental history of khawr rawri and khawr Al balid (dhofar, sultanate of Oman). *Palaeogeogr. Palaeoclimatol. Palaeoecol.* 213 (1–2), 1–36. doi:10.1016/j.palaeo.2004.03.014

Horisk, K. E., Ivory, S. J., McCorriston, J., McHale, M., Al Mehri, A., Anderson, A., et al. (2023). Vegetation dynamics in Dhofar, Oman, from the Late Holocene to present inferred from rock hyrax middens. *Quat. Res.* 116, 12–29. doi:10.1017/qua.2023.42

IPCC (2022). Climate change 2022: impacts, adaptation, and vulnerability," in *Contribution of working group II to the sixth assessment report of the intergovernmental panel on climate change*. Editors Pörtner, H.-O., Roberts, D. C., Tignor, M., Poloczanska, E. S., Mintenbeck, K., Alegría, A., et al. (Cambridge, UK and New York, NY, USA: Cambridge University Press. Cambridge University Press), 3056. doi:10.1017/9781009325844

Ivory, S. J., Cole, K. L., Anderson, R. S., Anderson, A., McCorriston, J., and Williams, J. (2021). Human landscape modification and expansion of tropical woodland in southern Arabia during the mid-Holocene from rock hyrax middens. *J. Biogeogr.* 48 (10), 2588–2603. doi:10.1111/jbi.14226

Kahmen, A., Hoffmann, B., Schefuß, E., Arndt, S. K., Cernusak, L. A., West, J. B., et al. (2013). Leaf water deuterium enrichment shapes leaf wax n-alkane δD values of angiosperm plants II: observational evidence and global implications. *Geochimica Cosmochimica Acta* 111, 50–63. doi:10.1016/j.gca.2012.09.004

Keeley, J. E., and Rundel, P. W. (2003). Evolution of CAM and C_4 carbon-concentrating mechanisms. *Int. J. Plant Sci.* 164 (S3), S55–S77. doi:10.1086/374192

Keeling, C. D. (1979). The Suess effect: ^{13}Carbon- ^{14}Carbon interrelations. *Environ. Int.* 2 (4–6), 229–300. doi:10.1016/0160-4120(79)90005-9

Killops, S. D., and Killops, V. J. (2013). *Introduction to organic geochemistry*. John Wiley and Sons.

Kwarteng, A. Y., Dorvlo, A. S., and Vijaya Kumar, G. T. (2009). Analysis of a 27-year rainfall data (1977-2003) in the Sultanate of Oman. *Int. J. Climatol.*, 29, 605–617. doi:10.1002/joc.1727

Lézine, A.-M., Bassinot, F., and Peterschmitt, J.-Y. (2014). Orbitally-induced changes of the Atlantic and Indian monsoons over the past 20,000 years: new insights based on the comparison of continental and marine records. *Bull. La Société Géologique Fr.* 185 (1), 3–12. doi:10.2113/gssgfbull.185.1.3

Lézine, A.-M., Ivory, S. J., Braconnot, P., and Marti, O. (2017). Timing of the southward retreat of the ITCZ at the end of the Holocene humid period in southern Arabia: data-model comparison. *Quat. Sci. Rev.* 164, 68–76. doi:10.1016/j.quascirev.2017.03.019

Lézine, A.-M., Saliège, J.-F., Mathieu, R., Tagliatela, T.-L., Mery, S., Charpentier, V., et al. (2002). Mangroves of Oman during the late Holocene; climatic implications and impact on human settlements. *Veg. Hist. Archaeobotany* 11 (3), 221–232. doi:10.1007/s003340200025

Lippi, M. M., Gonnelli, T., and Raffaelli, M. (2007). Pollen morphology of trees, shrubs and woody herbs of the coastal plain and the monsoon slopes of Dhofar (Sultanate of Oman). *Webbia* 62 (2), 245–260. doi:10.1080/00837792.2007.10670826

Liu, J., and An, Z. (2020). Leaf wax *n*-alkane carbon isotope values vary among major terrestrial plant groups: different responses to precipitation amount and temperature, and implications for paleoenvironmental reconstruction. *Earth-Science Rev.* 202, 103081. doi:10.1016/j.earscirev.2020.103081

Liu, W., and Yang, H. (2008). Multiple controls for the variability of hydrogen isotopic compositions in higher plant *n* -alkanes from modern ecosystems: variability of hydrogen isotopic compositions. *Glob. Change Biol.* 14 (9), 2166–2177. doi:10.1111/j.1365-2486.2008.01608.x

Maestre, F. T., Eldridge, D. J., Soliveres, S., Kéfi, S., Delgado-Baquerizo, M., Bowker, M. A., et al. (2016). Structure and functioning of dryland ecosystems in a changing world. *Annu. Rev. Ecol. Evol. Syst.* 47 (1), 215–237. doi:10.1146/annurev-ecolsys-121415-032311

McCorriston, J., Buffington, A., Olson, K., Martin, L., Abuazizeh, W., Everhart, T., et al. (2020). Ancient pastoral settlement in the dhofar mountains: archaeological excavations at shakil and halqoot. *J. Oman Stud.* 21, 152–171.

McCorriston, J., Moritz, M., Buffington, A., Pustovoytov, K., Ivory, S. J., and Abuazizeh, W. (2018). "Constructing the South arabian pastoral landscape," in *From Refugia to Oases. Acts of the 38th Rencontres Internationales d'Archéologie et d'Histoire d'Antibes Antibes: Éditions ADPCA*, 119–133.

Miller, A. G., and Morris, M. (1988). *Plants of dhofar, the southern region of Oman: traditional, economic, and medicinal uses* (Muscat, Oman: The Office of the Adviser for Conservation and the Environment, Diwan of Royal Court Sultanate of Oman).

Morrill, C., Overpeck, J. T., and Cole, J. E. (2003). A synthesis of abrupt changes in the Asian summer monsoon since the last deglaciation. *Holocene* 13 (4), 465–476. doi:10.1191/0959683603hl639ft

Nicholson, S. E. (2018). The ITCZ and the seasonal cycle over equatorial Africa. *Bull. Am. Meteorological Soc.* 99 (2), 337–348. doi:10.1175/bams-d-16-0287.1

Patzelt, A. (2015). Synopsis of the flora and vegetation of Oman, with special emphasis on patterns of plant endemism. *Abh. Braunschw. Wiss. Ges.* 282, 317.

Pedentchouk, N., Freeman, K. H., and Harris, N. B. (2006). Different response of δD values of n-alkanes, isoprenoids, and kerogen during thermal maturation. *Geochimica Cosmochimica Acta* 70 (8), 2063–2072. doi:10.1016/j.gca.2006.01.013

Peters, K. E., Walters, C. C., and Moldowan, J. M. (2005). *The biomarker guide*, 1. Cambridge, United Kingdom: Cambridge University Press. doi:10.1017/cbo9781107326040

Polissar, P. J., and D'Andrea, W. J. (2014). Uncertainty in paleohydrologic reconstructions from molecular δD values. *Geochimica Cosmochimica Acta* 129, 146–156. doi:10.1016/j.gca.2013.12.021

Polissar, P. J., and Freeman, K. H. (2010). Effects of aridity and vegetation on plant-wax δD in modern lake sediments. *Geochimica Cosmochimica Acta* 74 (20), 5785–5797. doi:10.1016/j.gca.2010.06.018

Rao, Z., Guo, W., Cao, J., Shi, F., Jiang, H., and Li, C. (2017). Relationship between the stable carbon isotopic composition of modern plants and surface soils and climate: a global review. *Earth-Science Rev.* 165, 110–119. doi:10.1016/j.earscirev.2016.12.007

Reimer, P. J., Austin, W. E. N., Bard, E., Bayliss, A., Blackwell, P. G., Bronk Ramsey, C., et al. (2020). The IntCal20 northern Hemisphere radiocarbon age calibration curve (0–55 cal kBP). *Radiocarbon* 62 (4), 725–757. doi:10.1017/RDC.2020.41

Renssen, H., Brovkin, V., Fichefet, T., and Goosse, H. (2003). Holocene climate instability during the termination of the african humid period. *Geophys. Res. Lett.* 30 (4), 2002GL016636. doi:10.1029/2002GL016636

Rozanski, K., Araguás-Araguás, L., and Gonfiantini, R. (1993). "Isotopic patterns in modern global precipitation," in *Geophysical monograph series*. Editors P. K. Swart, K. C. Lohmann, J. Mckenzie, and S. Savin (American Geophysical Union), 1–36. doi:10.1029/GM078p0001

Sachse, D., Billault, I., Bowen, G. J., Chikaraishi, Y., Dawson, T. E., Feakins, S. J., et al. (2012). Molecular paleohydrology: interpreting the hydrogen-isotopic composition of lipid biomarkers from photosynthesizing organisms. *Annu. Rev. Earth Planet. Sci.* 40 (1), 221–249. doi:10.1146/annurev-earth-042711-105535

Sage, R. F. (2004). The evolution of C_4 photosynthesis. *New Phytol.* 161 (2), 341–370. doi:10.1111/j.1469-8137.2004.00974.x

Sale, J. B. (1966). The habitat of the rock hyrax. *J. East Afr. Nat. Hist. Soc. Natl. Mus.* XXV, 2–214.

Scott, L., and Cooremans, B. (1992). Pollen in recent procavia (hyrax), petromus (dassie rat) and bird dung in South Africa. *J. Biogeogr.* 19 (2), 205. doi:10.2307/2845506

Scott, L., and Woodborne, S. (2007). Vegetation history inferred from pollen in Late Quaternary faecal deposits (hyraceum) in the Cape winter-rain region and its bearing on past climates in South Africa. *Quat. Sci. Rev.* 26 (7-8), 941–953. doi:10.1016/j.quascirev.2006.12.012

Sessions, A. L., and Hayes, J. M. (2005). Calculation of hydrogen isotopic fractionations in biogeochemical systems. *Geochimica Cosmochimica Acta* 69 (3), 593–597. doi:10.1016/j.gca.2004.08.005

Smith, F., Wing, S., and Freeman, K. (2007). Magnitude of the carbon isotope excursion at the Paleocene–Eocene thermal maximum: the role of plant community change. *Earth Planet. Sci. Lett.* 262 (1–2), 50–65. doi:10.1016/j.epsl.2007.07.021

Smith, F. A., and Freeman, K. H. (2006). Influence of physiology and climate on δD of leaf wax n-alkanes from C3 and C4 grasses. *Geochimica Cosmochimica Acta* 70 (5), 1172–1187. doi:10.1016/j.gca.2005.11.006

Strauch, G., Al-Mashaikhi, K. S., Bawain, A., Knöller, K., Friesen, J., and Müller, T. (2014). Stable H and O isotope variations reveal sources of recharge in Dhofar, Sultanate of Oman. *Isotopes Environ. Health Stud.* 50 (4), 475–490. doi:10.1080/10256016.2014.961451

Tipple, B. J., Berke, M. A., Doman, C. E., Khachaturyan, S., and Ehleringer, J. R. (2013). Leaf-wax *n* -alkanes record the plant–water environment at leaf flush. *Proc. Natl. Acad. Sci.* 110 (7), 2659–2664. doi:10.1073/pnas.1213875110

Wakeham, S. G., and Pease, T. K. (1992). *Lipid analysis in marine particles and sediment samples*. Savannah, GA: Skidaway Institute of Oceanography.